Title	Optical Second Harmonic Generation from Periodic Steps on Rutile TiO_2(110)
Author(s)	Takahashi, Hiroaki; Watanabe, Ryosuke; Mizutani, Goro
Citation	e-Journal of Surface Science and Nanotechnology, 8: 84-88
Issue Date	2010-02-27
Type	Journal Article
Text version	publisher
URL	http://hdl.handle.net/10119/9075
Rights	Copyright (C) 2010 The Surface Science Society of Japan. Hiroaki Takahashi, Ryosuke Watanabe, and Goro Mizutani, e-Journal of Surface Science and Nanotechnology, 8, 2010, 84-88. http://dx.doi.org/10.1380/ejssnt.2010.84
Description	

Japan Advanced Institute of Science and Technology

Optical Second Harmonic Generation from Periodic Steps on Rutile TiO$_2$(110)*

Hiroaki Takahashi,† Ryosuke Watanabe, and Goro Mizutani
School of Materials Science, Japan Advanced Institute of Science
and Technology, Asahidai 1-1, Nomi, Ishikawa 923-1292, Japan

We have succeeded in observing optical second harmonic generation (SHG) from steps on the TiO$_2$ surfaces adsorbed with HCOOH. The samples were single crystals of rutile TiO$_2$ with (110), (15 15 4), (13 9 0), and (671) faces. These samples underwent annealing in O$_2$ gas, HF etching, and immersion into HCOOH aqueous solution to adsorb HCOOH molecules on their surfaces. Their surfaces were characterized by reflection high energy electron diffraction (RHEED) and atomic force microscopy (AFM), and were confirmed to have regularly aligned steps created by the miscut of the samples. SH intensity as a function of the sample rotation angle was measured in air with the incident angle of 2° at the SH photon energy of $2\omega = 4.66$ eV. The SH intensity from the surfaces with steps were 2 to 3 orders of magnitude stronger than that from the (110) surface. The SH intensity patterns from these stepped surfaces were anisotropic. The result indicates that the contribution of the surface steps was observed selectively. [DOI: 10.1380/ejssnt.2010.84]

I. INTRODUCTION

A lot of efforts have been dedicated to the study of TiO$_2$ as a photocatalyst [1]. When we consider the mechanism of their catalytic reactions, the structures and electronic states of the TiO$_2$ surface forming the reaction field are important. Especially, active sites on the TiO$_2$ surface should play an essential role in the catalytic reactions. Surface defects of TiO$_2$ such as oxygen vacancies, steps, and kinks are known to be photocatalytic active sites [2, 3]. Hence, it is very important to clarify the structures and electronic states of the surface imperfections. In this study, we have focused our attention to the electronic states of step defects on the TiO$_2$ surface.

The electronic states of oxygen vacancies on the TiO$_2$ surface have been studied well by theoretical calculations [4–6], while theoretical or experimental studies of the electronic states at steps are rarely found in the literature. The reason for the poor numbers of experimental studies on the electronic states of surface defects including steps would be the difficulty in their selective measurement. In this work, we choose optical second harmonic generation (SHG) method [7–12] to measure the electronic states of steps on the TiO$_2$ surface selectively.

In the process of SHG, the light at frequency ω (fundamental light) is incident into media, and the light at frequency 2ω (SH light) is radiated from it. It is well known that the SHG occurs only in non-centrosymmetric media. For this reason, SHG is sensitive to the surfaces or interfaces of materials with centrosymmetric bulk structures. It has already been applied to the analyses of electronic states on the surfaces and interfaces [7–14]. Maeda *et al.* succeeded in measuring SHG from steps on the Au (887) and (443) single crystal surfaces[9]. This work motivated us to detect the electronic states of steps on the TiO$_2$

surface.

Rutile titanium dioxide has a centrosymmetric crystal structure. If the fundamental light is incident vertically onto the stepped surface, the oscillating direction of the electric field of the light is parallel to the terrace planes. When the fundamental electric field feels a broken symmetry, SHG occurs. The terraces, or the (110) surface, has 2-fold symmetry, and the electric field feels the same electronic response when it has a positive and negative amplitude. On the other hand, the (15 15 4) and (13 9 0) surfaces have mirror symmetry only and the (671) has no symmetry due to the existence of the steps. As a result, the electric field feels different responses when it has a positive and negative amplitude. Hence, it feels a broken symmetry only at the steps, and one can obtain the SH light with the contribution only of the steps. In this work, our objective is to detect the contribution of steps by comparing the SH response from three kinds of stepped surfaces, TiO$_2$ (15 15 4), (13 9 0), and (671), with that from a flat (110) surface in air. These three stepped surfaces are nearly (110) surfaces with surface miscut angles around 10°. The surfaces of all samples are adsorbed with formic acid molecules known as strong adsorbents on the TiO$_2$ surface [15], in order to avoid the direct adsorption of unidentified contamination from air.

II. EXPERIMENTAL

Single crystal substrates of rutile TiO$_2$ (110), (15 15 4), (13 9 0), and (671) purchased from Nakazumi Crystal Laboratory were used. They were immersed in 5% HF aqueous solution for 10 minutes and were annealed in O$_2$ gas at 800°C for 2 hours. Then, they were etched in HF aqueous solution again and were immediately dipped into 98% HCOOH solution for 15 minutes to adsorb HCOOH molecules on their surfaces. In order to characterize their surfaces, reflection high energy electron diffraction (RHEED) measurement was performed in 10^{-7}-10^{-8} Torr at room temperature, and atomic force microscopy (AFM) measurement was done in air at room temperature.

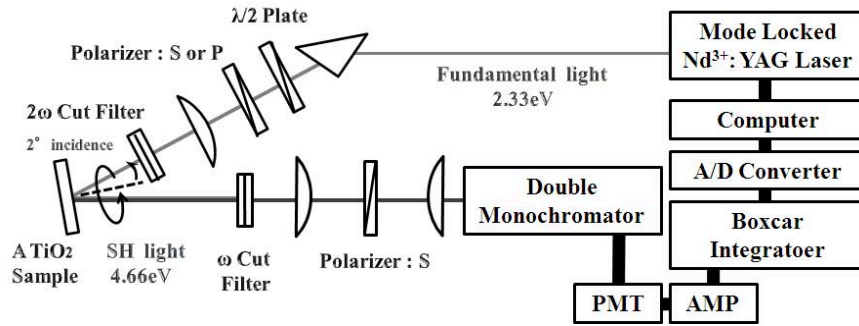The optical setup for the SHG measurement is shown in

FIG. 1: Optical setup for the SHG measurements. PMT and AMP represent photomultiplier and amplifier, respectively.
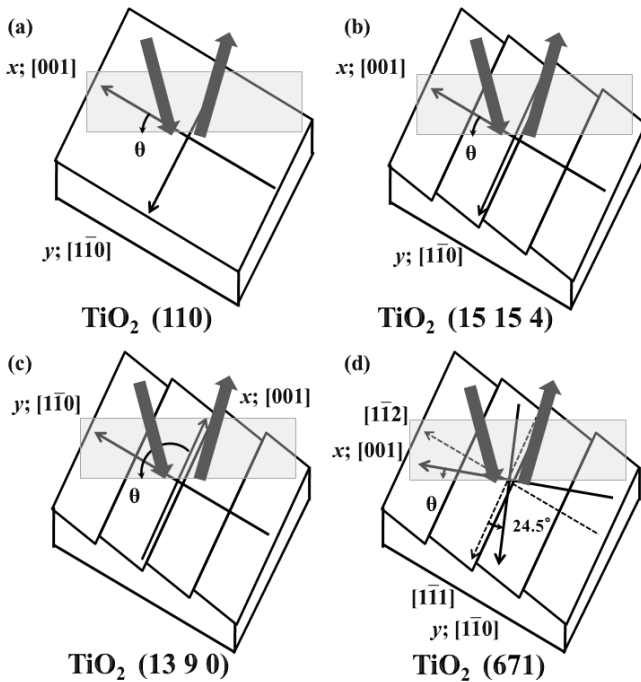

FIG. 2: Definition of the sample rotation angle for TiO$_2$ (a)(110), (b)(15 15 4), (c)(13 9 0), and (d)(671).

Fig. 1. The light source was a frequency-doubled mode-locked Nd^{3+}:YAG laser. The power of the incident fundamental light was kept at 120 μJ/pulse, and the incident angle was fixed at 2° with respect to the normal to the surfaces (z-axis). The sample was rotated around the z-axis, and the SH light intensity was measured at every 10° of the azimuthal angle. Definition of the sample rotation angle for each sample is shown in Fig. 2. The polarization of the fundamental light was either S or P, and that of the SH light was fixed to S. The fundamental and the SH photon energies were 2.33 eV and 4.66 eV, respectively.

III. RESULTS AND DISCUSSIONS

The AFM images of the samples are shown in Fig. 3. The high index TiO$_2$(15 15 4), (13 9 0), and (671) surfaces show regularly aligned steps. The intervals between the steps on the (15 15 4) and (671) surfaces were both

estimated as ∼40 nm from Figs. 3(b) and (d), and that on the (13 9 0) surface was estimated as ∼25 nm from Fig. 3(c). The height of the steps ranged from 3 to 5 nm, as a result of step bunching.

The RHEED patterns of the samples are shown in Fig. 4. The brighter spots in the RHEED patterns of the (110) surface in Fig. 4(a) and the (671) surface in Fig. 4(d) indicate (1×1) structures on the (110) surface terraces. The patterns attributed to steps are seen for the (15 15 4) and (13 9 0) surfaces in Figs. 4(b) and (c), respectively. Besides, these patterns imply that the (15 15 4) and (13 9 0) surfaces have the (110)(1×1) terraces as well. The periodicities of the steps on the (15 15 4) and (13 9 0) surfaces are estimated as ∼3 nm and ∼4 nm, respectively. These periodicities are different from those obtained from AFM images, i.e. 40 nm for the (15 15 4) surface and 25 nm for the (13 9 0) surface. Therefore, these surfaces are likely to have short and long periodic steps. We could not identify short periodic steps by AFM.

For the TiO$_2$(671) surface, no structures characteristic of short periodic steps were seen in the RHEED patterns, and thus the (671) surface is thought to consist only of long periodic steps. The height of the bunched steps on the (671) surface is estimated as ∼5 nm (∼15 ML) from its AFM image. The parameters determined by AFM and RHEED experiments are summarized in Table I.

According to the STM measurement of rutile TiO$_2$(110) by Diebold et al. [16], step edges running parallel to the ⟨001⟩ and ⟨1$\bar{1}$1⟩ directions were observed. The directions of these step edges are identical to those on the TiO$_2$ (13 9 0) and (671) surfaces. Therefore, we regarded them as the thermodynamically favorable and stable steps. Since step edges running parallel to the ⟨1$\bar{1}$0⟩ were never confirmed in the STM images, those on the (15 15 4) surface are thought to be thermodynamically unfavorable and unstable. According to this information, the faces of stable steps of TiO$_2$ should not be oriented in the [001] direction. The instability of the short periodic steps on the (15 15 4) surface may be reflected in the tilted streaks seen in Fig. 4(b). Regarding the bunched steps on the (15 15 4) surface, we also observed steps with step faces deviated from the [001] direction like the bunched steps on the (671) surface (not shown). These results indicate that both the short and long periodic steps on the (15 15 4) surface may contain stable steps like those on the (671) surface.

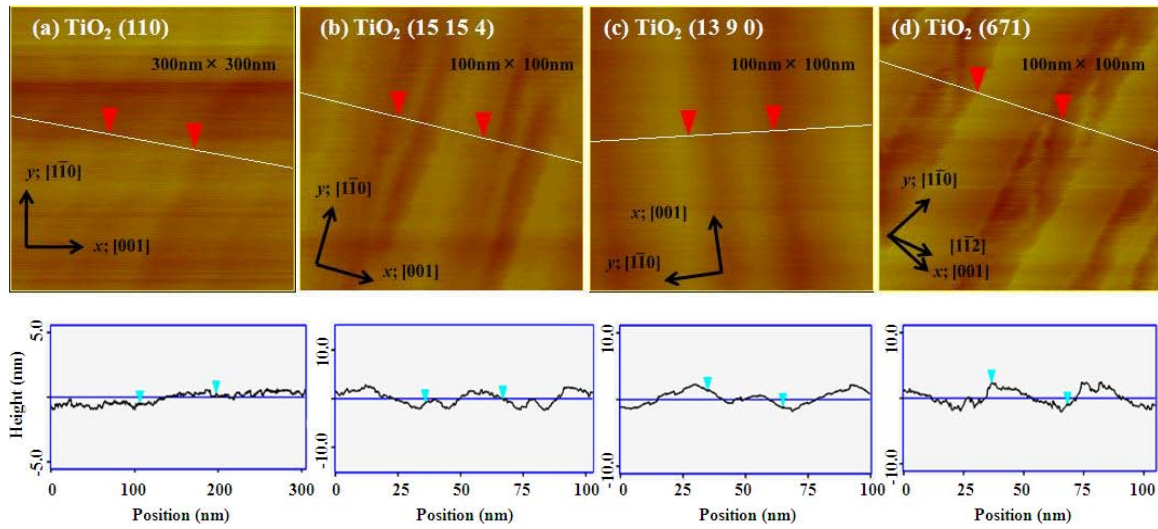The SH intensity patterns from all the samples as a

FIG. 3: AFM images of TiO$_2$ (a)(110), (b)(15 15 4), (c)(13 9 0), and (d)(671). The scanning areas were (a)300×300 nm^2 and (b),(c), and (d)100×100 nm^2. The panel below each AFM image shows the height profile along the white dashed line in the image.

TABLE I: Periodicity and height of the periodic steps.

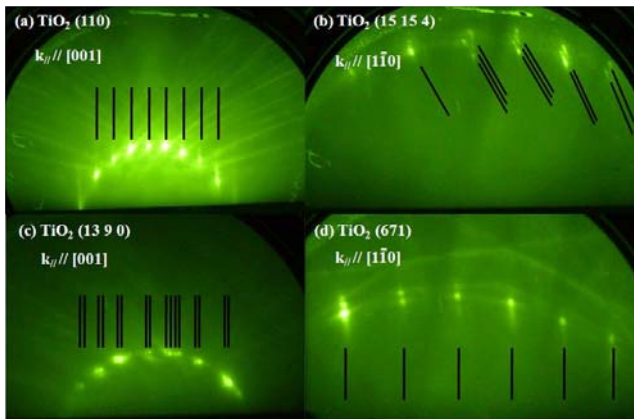|	TiO$_2$(15 15 4)	TiO$_2$(13 9 0)	TiO$_2$(671)
Periodicity of long periodic steps	∼40 nm	∼25 nm	∼40 nm
Height of long periodic steps	∼4 nm (∼12 ML)	∼3 nm (∼9 ML)	∼5 nm (∼15 ML)
Periodicity of short periodic steps	∼3 nm	∼4 nm	–

FIG. 4: RHEED patterns in high vacuum 10^{-7}-10^{-8} Torr at room temperature for TiO$_2$ (a)(110), (b)(15 15 4), (c)(13 9 0), and (d)(671).

TABLE II: Absolute values of fitted nonlinear susceptibility elements. The value of the most dominant component for each surface is written in bold.

	TiO$_2$(15 15 4)	TiO$_2$(13 9 0)	TiO$_2$(671)
$|\chi_{xxx}|$	3.01	–	1.56
$|\chi_{xyy}|$	**4.35**	–	**2.63**
$|\chi_{yxy}|$	2.12	–	0.17
$|\chi_{yyy}|$	–	1.32	0.68
$|\chi_{yxx}|$	–	0.95	0.23
$|\chi_{xxy}|$	–	**3.03**	2.05

function of the sample rotation angle around their surface normals are shown in Fig. 5. The SH intensity from the TiO$_2$ (110) surface was at the noise level as shown in Figs. 5(a) and (b). On the other hand, the signals from the high index surfaces show stronger SH intensity by 2 to 3 orders of magnitude as shown in Figs. 5(c) to (h). From the fact that the SH intensity is small enough from the (110) surface, we can disregard the contribution of the bulk higher order electromagnetic effect [8]. Thus, we attribute the difference in the SH intensity patterns

from different high index surfaces to the corresponding different surface steps.

Now, we compare the SH intensity patterns of the samples with each other. Firstly, we notice that the SH intensity patterns of the TiO$_2$(15 15 4) surface in Fig. 5(d) and the (671) surface in Fig. 5(h) for the polarization combination P in-S out have the same shapes as each other. Hence, similar electronic states may be detected in SH intensity patterns for the P in-S out polarization combination for the (15 15 4) and (671) surfaces. On the other hand, the SH intensity patterns of the (15 15 4) surface in Fig. 5(c) and the (671) surface in Fig. 5(g) for the polarization combination S in-S out are different. More asymmetric shape in Fig. 5(g) than in Fig. 5(c) is due to the lower symmetry of the (671) surface.

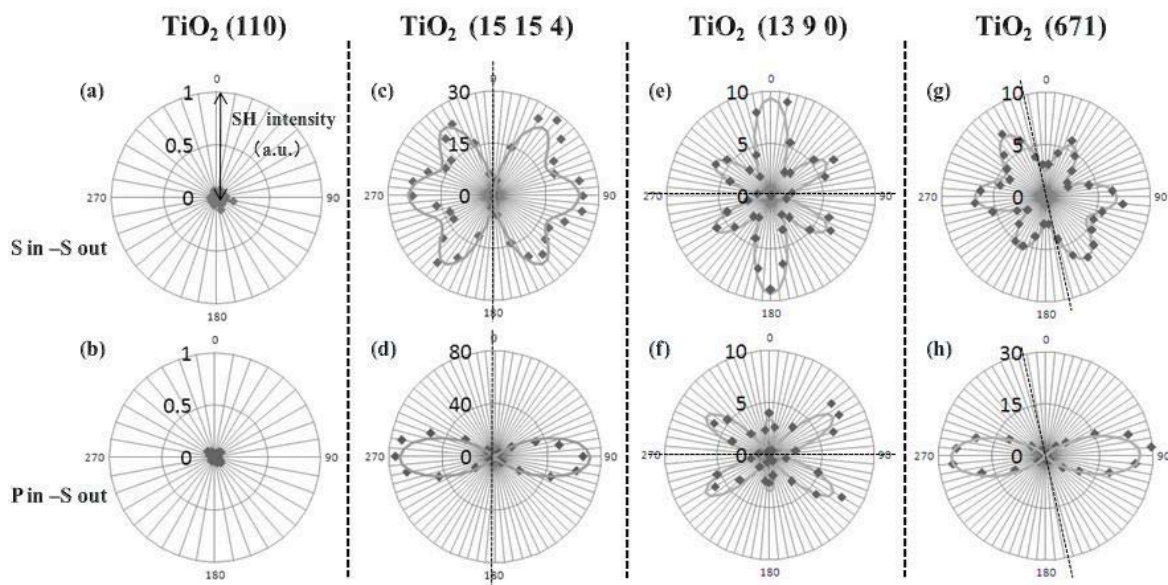We conducted a phenomenological pattern fitting for the experimental data of the TiO$_2$(15 15 4) surface in

FIG. 5: SH intensity patterns as a function of the sample rotation angle for the polarization combinations S in-S out and P in-S out. Dots represent experimental data, and curves represent phenomenologically fitted curves. Incident angle and photon energy were $2°$ and 2.33 eV, respectively. The dashed lines represent the sample rotation angles with SH electric field $E(2\omega)$ parallel to the step edges.

Figs. 5(c) and (d), and the (671) surface in Figs. 5(g) and (h) in order to analyze their electronic states in more detail [8]. We do not show the details of the process to obtain the fitted values here because it is complicated. The details of the fitting are described in ref. [8]. From the structural symmetry of these surfaces, non-zero susceptibility elements are $\chi_{xxx}^{(2)}$, $\chi_{xyy}^{(2)}$, and $\chi_{yxy}^{(2)}$ for the (15 15 4) surface, and $\chi_{xxx}^{(2)}$, $\chi_{xyy}^{(2)}$, $\chi_{yxy}^{(2)}$, $\chi_{xxy}^{(2)}$, $\chi_{yxx}^{(2)}$, and $\chi_{xxy}^{(2)}$ for the (671) surface. Here, x, y, and z represent [001], [1$\bar{1}$0], and [110] directions, respectively. By varying these nonlinear susceptibility elements as adjustable parameters, we obtained the fitted curves shown in Figs. 5(c), (d), (g), and (h), and the absolute values of the corresponding $\chi_{ijk}^{(2)}$ are shown in Table II.

As seen in Table II, the nonlinear susceptibility elements $\chi_{xyy}^{(2)}$ and $\chi_{xxx}^{(2)}$ for the TiO$_2$(15 15 4) and (671) surfaces are relatively larger than the other elements. The element $\chi_{xxy}^{(2)}$ arising from the broken symmetry in the y direction on the (671) surface also shows stronger contribution. Since only $\chi_{xyy}^{(2)}$ and $\chi_{yxx}^{(2)}$ strongly contribute to the SH intensity pattern for the P in-S out polarization combination, the similarity between the patterns in Fig. 5(d) and Fig. 5(h) should be due to the relation $|\chi_{xyy}^{(2)}| \gg |\chi_{yxx}^{(2)}|$ for the (671) surface. The first suffix of the dominant nonlinear susceptibility elements $\chi_{xyy}^{(2)}$, $\chi_{xxx}^{(2)}$, and $\chi_{xxy}^{(2)}$ for the (15 15 4) and (671) surfaces are all x. This result implies that the steps on these surfaces have strong nonlinear polarization in the x direction.

The SHG, AFM, and RHEED measurements imply that the steps on the (15 15 4) surface could have the structures basically composed of the ones on the (671) surface, and they have similar electronic states to each other. Because the steps on the (671) surface are reported to be stable, the (15 15 4) surface should contain the same

numbers of steps stable on the (671) and (761) surfaces. Each step on the (15 15 4) surface is expected to have finite $\chi_{xxy}^{(2)}$ value at the microscopic level because they are similar to the ones stable on the (671) and (761) surfaces. As the (15 15 4) surface has macroscopic mirror symmetry in the y direction, the macroscopic average of $\chi_{xxy}^{(2)}$ goes to zero.

Next, we focus on the SH intensity patterns of the TiO$_2$(13 9 0) surface shown in Figs. 5(e) and (f). These patterns are quite different from the ones of the (15 15 4) surface in Figs. 5(c) and (d), and the (671) surface in Figs. 5(g) and (h). This difference is considered to be mainly due to the difference in their miscut directions.

We have performed a phenomenological pattern fitting for the TiO$_2$(13 9 0) surface by varying the nonlinear susceptibility elements $\chi_{yyy}^{(2)}$, $\chi_{yxx}^{(2)}$, and $\chi_{xxy}^{(2)}$ as adjustable parameters. The fitted curves are shown in Figs. 5(e) and (f) and the absolute values of the corresponding $\chi_{ijk}^{(2)}$ are shown in Table II. In Table II, we see that the element $\chi_{xxy}^{(2)}$ is much larger than $\chi_{yyy}^{(2)}$ and $\chi_{yxx}^{(2)}$ for the (13 9 0) surface.

Let us discuss the origin of the dominant nonlinear susceptibility element $\chi_{xxy}^{(2)}$ for the TiO$_2$(13 9 0) surface. Since the faces of the steps on the (13 9 0) surface are the (1$\bar{1}$0) surfaces, they are equivalent to the (110) surface. For the (110) surface, the dominant nonlinear susceptibility element is reported to be $\chi_{113}^{(2)}$ in the notation of ref. [8] due to the electronic transitions in the Ti–O–Ti–O– chains containing surface bridging oxygen atoms [8], where 1 is the [001] direction and 3 is the [110] direction. This component corresponds to $\chi_{xxy}^{(2)}$ for the (13 9 0) surface in the present paper. Thus, we suggest that the electronic transitions in the bridging oxygen chains on the (1$\bar{1}$0) step faces may cause the optical nonlinearity of the

steps of the (13 9 0) surface.

IV. CONCLUSIONS

We prepared four kinds of single crystal rutile TiO_2 surfaces, (110), (15 15 4), (13 9 0), and (671), and characterized them by RHEED and AFM. Regularly aligned steps created by the miscut of the samples were observed on these vicinal surfaces. SHG measurement was performed using a nearly normal incident excitation beam. The SH intensity of the flat (110) surface was at the noise level, while that from the surfaces with steps were 2 to 3 orders of magnitude higher than that of the (110) surface. This fact indicates that we observed the contribu-

tion of steps separately by this SHG method. The SH intensity patterns for the P in-S out polarization combination from the (15 15 4) and (671) surfaces were similar to each other. This result was found to indicate a relation $|\chi^{(2)}_{xyy}| \gg |\chi^{(2)}_{yxx}|$ for the (671) surface from a phenomenological fitting with x and y in the [001] and $[1\bar{1}0]$ directions, respectively.

[1] A. Fujishima, X. Zhang, and D. A. Tryk, Surf. Sci. Rep. **63**, 515 (2008).

[2] X. Q. Gong, and A. Selloni, J. Catal. **249**, 134 (2007).

[3] A. Sirisuk, E. Klansorn, and P. Praserthdam, Catal. Commun. **9**, 1810 (2008).

[4] F. M. Hossain, G. E. Muech, L. Sheppard, and J. Nowotny, Solid State Ionics **178**, 319 (2007).

[5] C. Di Valentin, G. Pacchioni, and A. Selloni, Phys. Rev. Lett. **97**, 166803 (2006).

[6] N. Yu, and J. W. Halley, Phys. Rev. B **51**, 4768 (1995).

[7] A. N. Shultz, W. Jang, W. M. Hetherington III, D. R. Bear, L.-Q. Wang, and M. H. Engelhard, Surf. Sci. **339**, 114 (1995).

[8] M. Omote, H. Kitaoka, E. Kobayashi, O. Suzuki, K. Aratake, H. Sano, G. Mizutani, W. Wolf, and R. Podloucky, J. Phys.: Condens. Matter **17**, S175 (2005).

[9] Y. Maeda, T. Iwai, Y. Satake, K. Fujii, S. Miyatake, D. Miyazaki, and G. Mizutani, Phys. Rev. B **78**, 075440 (2008).

[10] T. F. Heinz, F. J. Himpsel, and E. Burstein, Phys. Rev. Lett. **63**, 644 (1989).

[11] S. Nakamura, K. Matsuda, T. Wakasugi, E. Kobayashi, G. Mizutani, S. Ushioda, T. Sekiya, and S. Kurita, J. Luminescence **87-89**, 862 (2000).

[12] E. Kobayashi, T. Wakasugi, G. Mizutani, and S. Ushioda, Surf. Sci. **402**, 537 (1998).

[13] E. Kobayashi, K. Matsuda, G. Mizutani, and S. Ushioda, Surf. Sci. **427**, 294 (1999).

[14] G. Mizutani, J. Kameya, N. Ishibashi, S. Tanaka, T. Sekiya, and S. Kurita, Recent Res. Devel. Optics **3**, 649 (2003).

[15] T. Tan, D. Beydoun, and R. Amal, J. Photochem. and Photobiol. A: Chem. **159**, 273 (2003).

[16] U. Diebold, J. Lehman, T. Mahmoud, M. Kuhn, G. Leonardelli, W. Hebenstreit , M. Schmid, and P. Varga, Surf. Sci. **411**, 137 (1998).